The United Nations University

GEOTHERMAL TRAINING PROGRAMME
Orkustofnun, Grensásvegur 9,
IS-108 Reykjavík, Iceland

Reports 1998
Number 10

GEOCHEMICAL CHARACTERISTICS OF THERMAL FLUID FROM THE XIAOTANGSHANG GEOTHERMAL FIELD, BEIJING, CHINA

Pan Xiaoping
Beijing Geologic Engineering Survey Institute
Beijing Geothermal Research and Development Centre
No 38 Bei Wa Road, Fu Wai Ba Li Zhuang,
Beijing,
P.R. CHINA

ABSTRACT

The Xiaotangshan geothermal field is a famous low-temperature geothermal field in China. Its geothermal resources have been utilized for a long time but utilization of hot water from boreholes began 25 years ago. The geothermal system consists basically of three reservoirs, Jx.w and Jx.t made of dolomite and the Cambrian system made of limestone. The present study indicates that the thermal water is of meteoric origin and its age, based on ^{14}C dating, is approximately 24,000 to 30,000 years. The study shows that the chemical composition of waters from three monitoring wells has changed very little during exploitation. It is suggested that as long as the reservoirs are exploited similarly as between 1987 and 1995, only minor chemical changes will occur. Because of the relatively low temperature of the geothermal water and mixing with cold groundwater, the thermal fluid seems not to be in equilibrium with any hydrothermal minerals in the reservoirs, except for chalcedony. Geothermometer calculations show that one can expect the highest temperature, approximately 80°C, in the eastern part of the geothermal field. Therefore, the main potential for further development of the geothermal resources is in that area. The data of ^{14}C dating, chemical and temperature changes, and geology and tectonics indicate that the flow direction of the thermal fluid is from north to south and the thermal fluid is mixed with cold water in the north.

1. INTRODUCTION

The Xiaotangshan geothermal field is located in a northern suburb, 25 km from the centre of Beijing in China (Figure 1). The initial Xiaotangshan hot spring is believed to be more than 700 years old with a temperature of 52°C. The spring, famous in ancient China, is listed in many historic books. Emperors and nobles of feudal dynasties of past ages often went to the hot spring to take baths. Empress Dowager CIXI of the QING dynasty built an imperial palace with a special bathing pool. The palace was destroyed by bombs from Japanese planes in the second world war, so only ruins remain. Local residents have used the spring for bathing and washing, and herdsmen came from Mongolia grasslands to take baths for "healing every disease" (Zheng, 1991).

The Beijing Hydrogeological Team (the former name of Beijing Geologic Engineering Survey Institute) of the Ministry of Geology carried out a geothermal survey and drilled some exploration wells between 1956 and 1958. The survey indicated a surface extent of hot springs of about 0.6 km^2. Long term monitoring, including flow rate, temperature and water chemistry, started then. In the early 1970's, the Hydrogeological Team and concerned units commenced an extended exploration. As a result, the development and utilization of the geothermal resources were extended. So far, boreholes in the geothermal field have been exploited for more than 25 years.

FIGURE 1: Location of the Xiaotangshan field

The present study is based on the analyses of fluid samples and the results of previous work in the geothermal field. The main objectives are as follows:

To evaluate chemical characteristics of the thermal fluid;
To determine the origin, age and movement of the thermal fluid;
To distinguish and classify thermal fluids from different reservoirs;
To determine if mixing takes place between water types;
To estimate reservoir temperatures of the field by means of various geothermometers;
To analyse the main chemical and temperature changes since utilization started.

2. GEOLOGICAL AND HYDROLOGICAL SETTING

2.1 Geological setting

The basement rock formations in the Xiaotangshan geothermal field are controlled by complicated geological structures and they are older in the north than in the south. A Quaternary formation covers most of the geothermal field, consisting of 0-500 m of sand or clay. In general, the bottom section consists of very fine clay. Figure 2 shows a geological and structural map of the field. The rock outcrop occurring at the Xiaotangshan Sanatorium in the northern part consists of dolomite of the Wumishan formation (Jx.w) which belongs to the Jixian system (name of China's standard formation profile). The Jx.w formation consists of sedimentary rocks with a thickness of more than 2000 m in the Beijing area. So far, no single borehole has penetrated all the formation in the Xiaotangshan field, but sediments upto 700 m have been drilled. The Jx.w formation is about 1.2-1.4 billion years (BY) of Mid-Upper Proterozoic era. Then successively, the Hongshuizhuang formation, which is shale, is about 80 m thick. The Tieling formation (Jx.t), which is about 1.0-1.2 BY, consists of dolomite and its thickness is about 350 m. The Qingbaikou system, which is 0.8-1.0 BY, is limestone and shale and in the range0-600 m in different areas in the field. The Cambrian system, which is 500-570 million years old, consists of limestone. Its thickness increases from north to south and reaches 800 m in the southern part of the field. The Jurassic system, which is 136-190 MY, is made of volcanic rocks. The formation has been found in geothermal boreholes in the southern and eastern parts of the field (Pan et al., 1997).

2.2 Structural features

Due to crustal movements the geological structure of the area is very complicated, with a number of faults and folds. In some areas the basement rocks are severely folded so that groups of formations that can be found in one place are lacking in another. Geological structures control the distribution and thickness of the formations. The major faults in the field are listed in Table 1 (Pan et al., 1997).

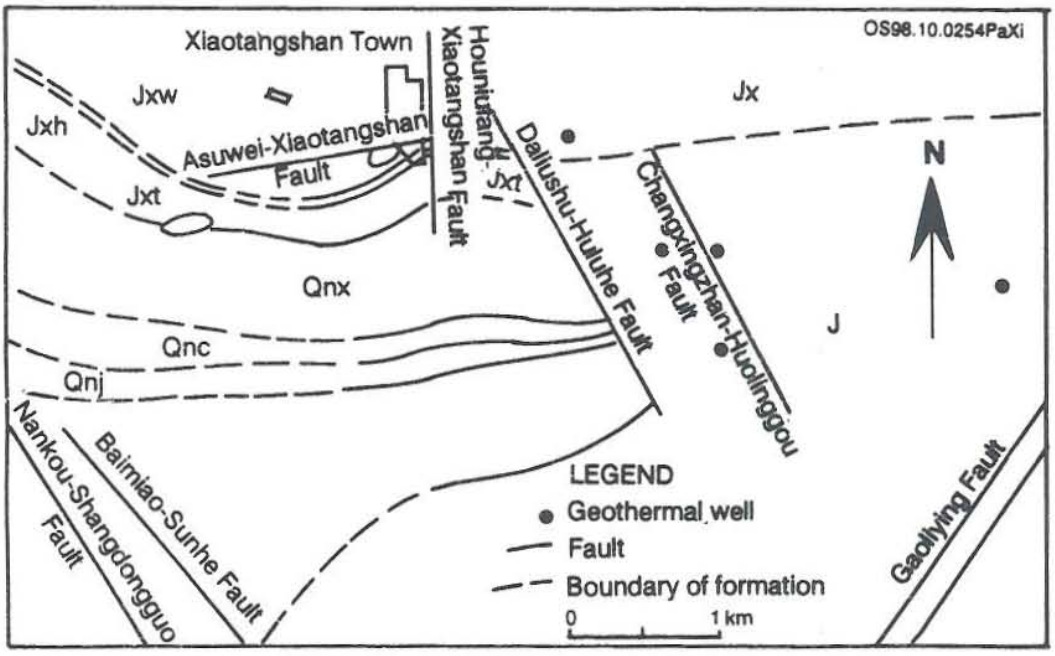

FIGURE 2: Geological and structural map of the Xiaotangshan field

TABLE 1: Major faults in the Xiaotangshan geothermal field

No.	Name	Character		Strike	Length (km)	Evidence
		Up	Down			
1	Asuwei-Xiaotangshan fault	N-block	S-block	NEE	3.5	Data from boreholes, granite intrusion
2	Daliushu-Huluhe fault	W-block	S-block	NW	3.5	Data from boreholes and the intensive belt of gravity isolines
3	Houniufang-Xiaotangshan fault	W-block	S-block	NS	4.0	Data from boreholes; intensive belt of electric resistivity isolines
4	Changxingzhan-Huolinggou fault	W-block	S-block	NW	2.5	Data from boreholes and geophysics
5	Gaoliying fault	W-block	N-block	NE		Data from gravitation and electrical resistivity sounding
6	Nanlou-Shangdongguo fault	NS-block	SW-block	NW	17.5	Data from boreholes and intensive belt of gravity isolines

2.3 Hydrological conditions

As pointed out previously the geothermal system at Xiaotangshan consists of three separated reservoirs called the Jx.w, Jx.t and Cambrian systems. The Jx.w and Jx.t reservoirs are made of dolomite, and the Cambrian reservoir consists of limestone. By volume the Jx.w reservoir is the largest of the three reservoirs, then the Cambrian system, and Jx.t is the smallest. The dolomites and limestones are very inhomogeneous with respect to porosity and permeability. The porosity of Jx.w is in the range of 0.2-1.5%, Jx.t 0.3-1.5%, and Cambrian system 0.4 -1.2%. In the eastern and southern parts of the geothermal field, the Cambrian system is overlain directly by the Jx.w because the Hougshuizhuang, Jx.t and Qinbaikou formations are lacking due to tectonic movements. Based on pump tests of geothermal wells of the geothermal field, the Jx.w and Cambrian systems can be looked upon as the same reservoir.

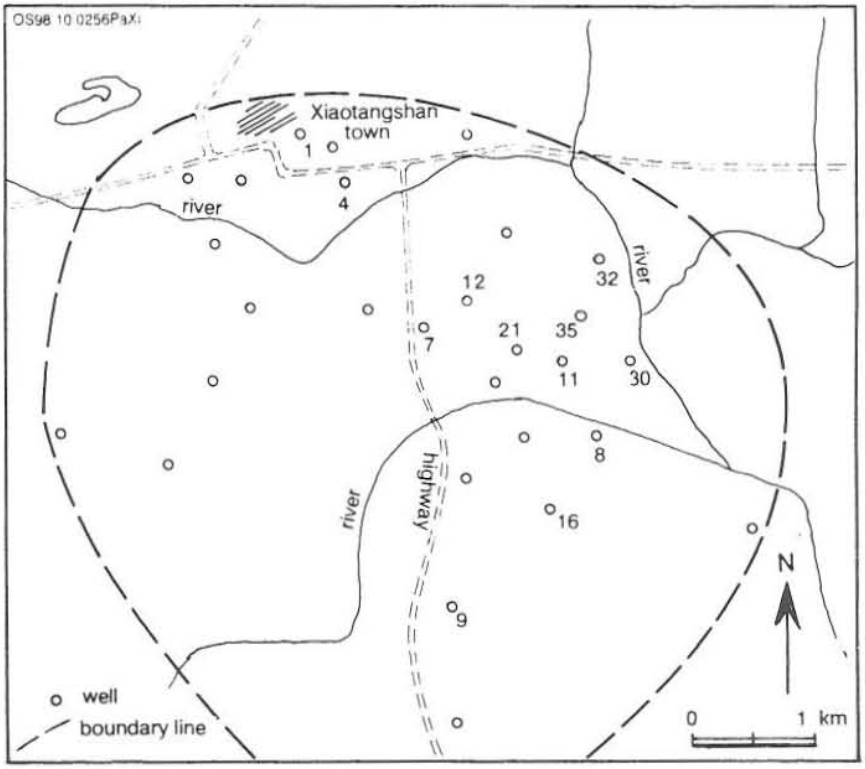

FIGURE 3: The extent of the Xiaotangshan field and location of wells

The Hougshuizhuang, Qinbaikou, Jurassic system and Quaternary formations are aquicludes or cap rocks. The Qinbaikou formations are layers of limestone and sandstone up to 80 m thick, but their porosity and permeability are so small that they act as aquicludes. The bottom of the Quaternary formation is fine clay which is aquiclude, too (Pan et al., 1997).

2.4 Subsurface temperature

There is a clear indication that the distribution of subsurface temperature is controlled by conductive thermal faults. Isothermal maps at depths of 500 and 1000 m indicate that there are two areas of higher than normal temperature. One is located in the northwestern part of the field, close to the town of Xiaotangshan and the other is in the eastern part, around wells 21 and 30 (Figure 3). At 1000 m the highest temperature is about 60°C in the northwestern part and 65°C in the eastern part. The Asuwei-Xiaotangshan fault in the northwest district and the Daoliushu-Huluhe fault in the southeast district are conductive thermal faults. At present the Daoliushu-Huluhe fault is thought to be an active conductive fault. The fault has higher heat conductivity and transmissivity than the Asuwei-Xiaotangshan fault. Boreholes, geophysical and geochemical data have proved that the Daliushu-Huluhe fault is an important fault controlling reservoir temperature and stratigraphy. There are higher reservoir temperatures, productivity and transmissibility nearby on both sides of the fault.

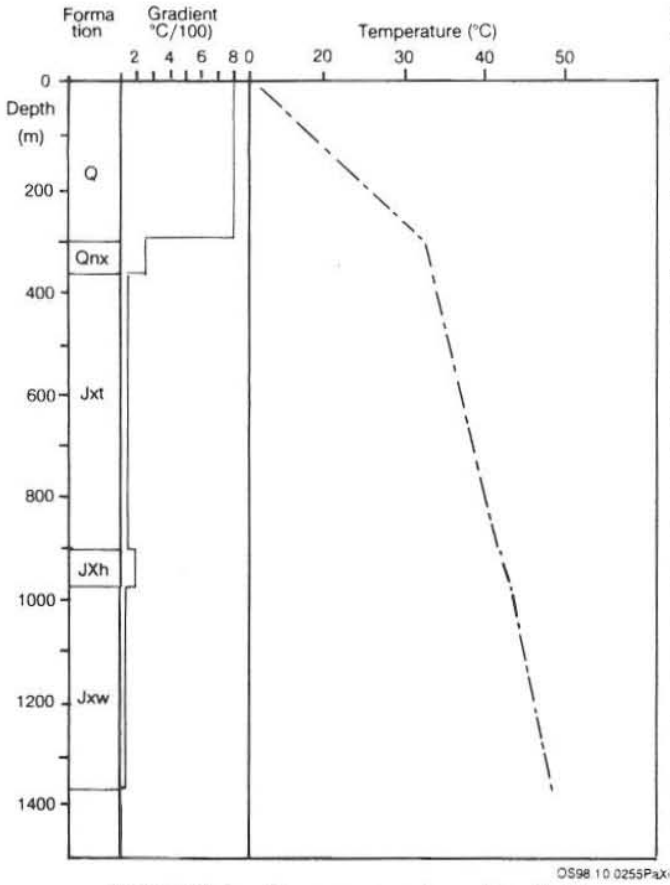

FIGURE 4: Temperature log of well 12, Xiaotangshan field

Another feature that affects the subsurface temperature is that different formations have different temperature gradients. Temperature gradients in reservoirs are lower than in aquicludes. Figure 4 shows a temperature log from well 12. In the geothermal field the order of formation from top to bottom is Quaternary formation, Jurassic system, Cambrian system, Qingbaikon system and Jixian system. No single borehole has penetrated all the formations due to their distribution

and the limited depth of the boreholes and Table 2 shows temperature gradients of reservoirs and aquicludes. Temperature gradients of reservoirs range from 1.29 to 2.16°C/100 m, and for aquicludes from 3.21 to 4.06°C/100 m.

TABLE 2: Temperature gradient of reservoirs and aquicludes, Xiaotangshan field

Well no.	Temperature gradient of aquicludes (°C/100 m)				Temperature gradient of reservoirs (°C/100 m)		
	Q	J	Qin.	Hong.	Cambrian	Jx.t	Jx.w
27	2.44		6.34			1.63	
28	4.38						
29	3.43						
30		1.74					2.33
31		2.01			0.63		
32		1.25			1.32		0.45
33			3.05	2.21		1.47	2.04
34		11.56		2.43		2.04	1.00
35					3.13		2.58
36		1.01			1.6		
37			2.78	2.78		0.45	
38	2.49				1.09		0.85
39	5.22						1.07
40	4.56				1.38		0.39
41					2.86	5.2	0.86
Average	**3.75**	**3.51**	**4.06**	**3.21**	**1.83**	**2.16**	**1.29**

Qin: Qingbakou System; Hong: Hongshuizhuan formation.

3. EXPLORATION MANAGEMENT AND UTILIZATION OF GEOTHERMAL RESOURCES

3.1 Exploration and management of geothermal resources

The Xiaotangshan geothermal field used to be a natural hot spring area with a total of eleven hot springs. The thermal fluid had temperatures of 22-52°C. Its natural artesian flow was 6,211 m^3 per day measured during the survey in 1956. There are some isolated low hills to the north and a wide expanse of flat land with a river flowing across the southern part of the field. Hot springs gushed out from the feet of these hills (Xiaotangshan) and discharged towards the south, either by flowing into a stream or seeping into the ground. At the beginning of the 1970's, a number of irrigation wells were drilled in the area in order to extract vast amounts of shallow groundwater. This lowered the regional groundwater level so most of the hot springs did not gush out at the surface but flowed as groundwater towards the south. At that time the total artesian flow decreased to about 1,000 m^3 per day. In order to utilize the geothermal resources, some users began to explore and drill geothermal wells under the guidance of geological departments. The first successful geothermal well was drilled outside of the hot spring area in 1974. As a result, the hot springs dried up one by one so users had to drill new wells to find geothermal fluid. Geothermal users shared the exploration risk and drilling cost with the geological departments, due to a lack of national exploration input. Once the well was drilled, the user of it owned and utilized the well

for individual purposes. Such a developing scheme accelerated the regional drawdown of the field.

During the developmental period, a resolution for strengthening exploitation, development, research, and management of geothermal resources was passed at a Mayor's working Meeting of the Beijing Municipal Government in September of 1984. The resolution gave Beijing's Municipal Government power to regulate and manage geothermal resources under the department of Administration of Beijing's Geothermal Resources which is located in the Bureau of Geology and Mineral Resources. Under this new plan, all new wells and existing production wells have to be examined by that department in order to get approval. In 1986, this department instituted a compensation fee for geothermal water paid by well owners. In 1991, annual quotas were allocated to each geothermal user to help regulate use and to reduce waste. The user is rewarded when staying within the annual quota or when a saving is shown. On the other hand, users receive penalties when waste occurs or they go over the annual quota. Because of this new unified management and the enactment and enforcement of these regulations by the Administration of Geothermal Resources, the geothermal reservoirs in the extended geothermal field of about 44 km^2 have a greater opportunity of surviving depletion from exploitation (Zheng, K., at el.,1997).

3.2 The extent of the geothermal field

The geothermal resource standard of China states that suitable utilization of geothermal resources are reservoirs of depth less than 2000 m and with discharge temperature higher than 40°C. Based on that, data from boreholes, tectonics, geology, geophysics and geochemistry were used to ascertain the size of the field area, i.e. 44 km^2. The extent and borehole locations are shown in Figure 3 (Pan, 1995).

3.3 Geothermal utilization

The annual exploited yield of thermal water from the Xiaotangshan geothermal field has reached more than 4 million m^3 since 1989. The different types of utilization of geothermal resources of the field are shown in Table 3. The thermal fluid is utilized directly for bathing, swimming, space heating, greenhouses, fish farming, convalescing and recuperation (C and R). There are 7 large fish farms using geothermal water in the field. It takes at least two years for fish to grow up after hatching to market size at natural conditions. Fish cannot be hatched until May in the Beijing district, however, it can be hatched in January or February if water in the fish pool is heated with geothermal water to 14°C for carp or shrimp and 17°C for African fish types. The seven fish farms can provide large number of fry to other fish farms in Beijing or other districts in March or April every year. It takes 7 months for fry to grow up, so with the help of geothermal water it only takes one year to grow fish from hatching to market size.

The composition of the geothermal fluid is in many ways useful to cure diseases. For example the concentration of fluoride is about 5-8 mg/l, boron about 0.2 mg/l, and radioactive elements occur in low concentrations: Rn about 110 bq/l, Ra about 1.5×10^{-12} g/l, U about 6×10^{-8} g/l. Chinese medicine theory and actual results have proved that thermal fluid can cure or prevent many different diseases. The Xiaotangshan, sanatorium built in the 1950's, has been the main coordinator in China to use thermal water to cure diseases for a large number of patients. Table 4 shows the curative effect of the thermal fluid. The data is from the Xiaotangshan sanatorium.

TABLE 3: Utilization of geothermal resources in the Xiaotangshan geothermal field

User	Well No.	Reservoir	Temperature (°C)	Utilization project	Statistics
1	1	Jx.w	53.8	Space heating	60,000 m^2
	2	Jx.w	54.5		
	6	Jx.w	46	C and R, bathing	3,200 P/D

User	Well No.	Reservoir	Temperature (°C)	Utilization project	Statistics
2	5	Jx.t	42.0	Fish farming, bathing	66,000 m^2 100 P/D
	19	Jx.t	39.0		
	26	Jx.w	43.2		
	28	Cambrian	51.5		
3	46	Jx.w	51	Bathing	350 P/D
4	12	Jx.w	53.3	Space heating	1,500 m^2
	13	Jx.t	51.5	Greenhouses	33,000 m^2
	27	Jx.t	51.0		
5	4	Jx.t	48.5	Fish farming, space heating	33,000 m^2 1,000 m^2
	18	Jx.t	48.5		
	23	Jx.t	47.5		
6	11	Cambrian	67.4	Space heating swimming	15,000 m^2 1,000 P/D
7	22	Jx,t	58	Space heating	20,000 m^2
8	8	Cambrian	52.5	Bathing	800 P/D
9		Cambrian	43.7	Bathing	600 P/D
10	42	Jx.w	54	Bathing space heating	500 P/D 16,200 m^2
11	16	Cambrian	42	Bathing, C and R	200 P/D
12	30	Jx.w	70	Fish farming, greenhouses, bathing	66,000 m^2 19,800 m^2 200 D/P
	32	Jx.w	58		
13	20	Jx.w	50.5	Space heating, bathing	10,000 m^2,100 P/D
14	7	Jx.t	59.5	Greenhouses, bathing	33,000 m^2 100 P/D
	37	Jx.w	56		
15	46	Jx.t	48	Fish farming, bathing	6,600 m^2, 200 P/D
16	17	Cambrian	46.5	Greenhouses fish farming	6,600 m^2 3,300 m^2
17	33	Jx.w	48.3	Fish farming	33,000 m^2
18	45	Jx.w	51	Swimming	1,000 P/D
19	39	Jx.w	49	Fish farming	6,600 m^2

P/D: persons per day; C and R: convalescing and recuperation.

TABLE 4: Convalescing and recuperation effects of the thermal fluid

Disease	Observed patients	Cure or notable curative effective	Effective	Not effective	Effectiveness (%)
Psoriasis	205	90	93	22	89.3
Neurodermatitis	173	60	96	17	90.2
Chronic eczema	168	72	70	26	84.5
Rheumarthritis	278	108	142	28	89.9
Bone arthritis	677	4	601	72	89.4
Coronary heart disease	129	26	100	27	79.1
Hypertension	1826	129	1532	185	90.0
Chronic gastritis	741	71	598	72	90.3
Neurosis	4202	318	3434	452	89.3

4. SAMPLING, ANALYSIS AND RESULTS

4.1 Sampling

Every well was sampled for geothermal water at the end of a pump test when drilling had finished. Three wells, one from each reservoir, were selected for chemical monitoring. They are well 1 for the Jx.w reservoir, well 7 for the Jx.t reservoir and well 9 for the Cambrian system. Until 1985 several samples were collected from each of the wells. But since 1985 samples have been collected twice a year. The first sample is taken in March, after intensive exploitation during the winter season, and the second one at the end of October after much less exploitation during spring and summer.

4.2 Analytical methods

All water samples are sent to the Beijing water quality analytical centre laboratory which has a national qualification on water analysis. Samples for Fe analyses are acidified with HCl during sampling to prevent $Fe(OH)_3$ precipitation. The analytical methods at the laboratory are listed in Table 5. The ^{14}C samples were analysed by the ^{14}C analytical laboratory at the National Seismic Institute. The institute belongs to the Chinese Academy of Sciences.

TABLE 5: Chemical analytical techniques for the thermal fluid

Composition	Method of analysis
CO_2	Alkalimetry-titration
H_2S	Titration
B	Spectrophotometry
SiO_2	Spectrophotometry
Na	Atomic absorption spectrometry
K	Atomic absorption spectrometry
Mg	Atomic absorption spectrometry
Ca	Atomic absorption spectrometry
F	Ion selective electrode
Cl	Ion chromatography
SO_4	Ion chromatography
Al	Atomic absorption spectrometry
Fe	Atomic absorption spectrometry
NO_3	Spectrometry
^{18}O	Mass spectrometry
D	Mass spectrometry
pH	Ion selective electrode

4.3 Results of chemical analysis

Results of the chemical analyses from the three monitoring wells are listed in Tables 6, 7 and 8 for wells 1, 7 and 9, respectively. Table 9 shows results of chemical analysis from several different wells, including one sample from each of the monitoring wells.

TABLE 6: Analytical results of major constituents in water from well 1 of the Jx.w reservoir (mg/l)

No.	Date	K	Na	Ca	Mg	Fe	Cl	HCO_3	SO_4	HBO_2	H_2S	SiO_2	F	pH
1	29.01.75	14.06	84.55	41.68	15.08	0.94	33.32	280.69	43.23	0.76	0.11	44.2	8.7	8.3
2	01.03.75	15.05	86.25	42.08	14.84	0.18	34.03	280.69	145.05	1.40	0.17	44.8	6.17	8.1
3	04.06.76	14.55	83.32	42.284	15.69	0.18	32.26	294.12	73.486	0.40	-	40.0	5.00	7.3
4	29.03.79	12.40	75.00	41.70	15.40	0.50	29.80	286.80	80.20	0.20	-	32.0	6.00	7.4
5	11.06.79	14.00	84.20	42.30	14.80	0.34	32.30	280.70	75.40	0.20	-	37.5	6.20	7.3
6	18.08.79	13.60	82.80	43.90	19.30	0.28	31.60	283.10	96.10	0.20	0.49	37.0	6.00	7.2
7	24.09.80	15.10	87.20	40.10	14.80	0.16	31.90	275.80	74.90	5.00	0.06	40.0	6.60	7.6
8	12.03.82	11.88	94.75	41.28	16.66	0.11	28.37	286.79	91.74	1.36	-	32.0	8.00	7.8
9	20.10.82	14.40	82.00	42.10	21.90	0.40	28.40	284.40	96.10	0.80	0.08	35.0	6.50	7.8
10	04.11.83	13.33	86.67	40.33	14.67	1.70	22.80	291.70	72.80	0.12	-	32.0	6.32	7.7
11	14.03.84	14.00	84.44	42.17	14.36	0.12	27.72	280.70	78.30	1.20	-	32.0	6.40	7.5
12	21.06.84	14.18	81.39	42.17	15.03	0.14	24.36	286.80	72.00	0.80	-	35.0	5.40	7.6
13	11.09.84	14.38	76.30	43.82	14.58	0.26	26.77	285.60	77.60	1.20	-	38.0	5.96	7.4
14	02.04.85	13.86	77.50	41.43	14.92	0.25	24.34	279.50	62.60	1.20	-	35.0	6.15	7.53
15	15.06.85	14.40	80.80	42.17	14.73	0.10	23.01	244.08	59.87	1.28	-	37.0	5.74	8.52
16	27.11.85	14.10	72.40	43.45	15.18	0.39	23.60	278.20	76.30	1.04	-	34.0	6.80	7.7
17	23.10.86	14.46	79.86	42.53	15.47	0.20	27.30	275.80	71.40	1.12	0.14	33.0	6.49	7.6
18	24.03.87	12.90	77.40	43.63	16.13	0.32	26.90	290.46	66.40	1.60	0.14	34.0	6.29	7.5
19	07.11.87	12.90	71.50	44.18	15.62	0.19	26.70	290.46	72.10	0.96	0.05	33.0	6.64	7.5
20	14.03.88	12.50	74.10	44.00	15.62	0.14	25.30	290.46	64.10	1.52	0.19	33.0	5.50	6.9
21	01.11.88	10.70	77.90	43.08	15.77	0.28	25.90	292.90	77.90	0.96	0.11	28.0	6.03	7.34
22	05.04.89	13.90	76.70	44.00	15.73	0.40	25.30	292.89	65.70	1.12	0.07	30.0	5.81	7.22
23	22.11.89	12.70	77.50	43.82	15.69	0.10	26.60	292.89	68.60	1.50	0.08	33.0	5.27	7.54
24	19.03 90	15.10	79.50	44.00	16.13	0.23	26.10	286.79	66.90	1.20	-	35.0	5.95	7.52
25	20.11.90	14.60	81.20	43.45	16.13	0.16	26.40	292.89	66.00	1.40	-	39.0	6.16	8.08
26	14.03.91	13.70	80.00	44.18	16.06	0.12	26.80	292.89	65.70	2.00	0.06	33.0	6.00	7.48
27	22.10.91	11.90	74.20	43.45	16.28	0.114	25.30	286.78	62.60	1.10	0.06	40.0	6.20	7.38
28	16.03.92	12.90	81.60	44.92	16.65	0.24	27.00	298.98	66.90	1.20	-	35.0	6.40	7.46
29	19.11.92	12.46	72.00	43.45	16.13	0.31	24.80	292.88	65.80	1.20	-	31.0	6.30	7.5
30	16.03.93	12.57	77.77	43.63	15.99	0.20	24.81	298.98	67.38	1.50	-	32.0	6.00	7.47
31	26.11.93	11.60	73.64	43.45	16.54	0.30	25.54	298.98	59.51	2.0	0.10	30.0	25.54	7.45
32	08.04.94	17.25	81.92	41.25	14.57	0.27	26.95	292.90	67.61	1.50	-	31.0	6.30	7.92
33	05.11.94	13.64	78.18	42.17	16.54	0.31	25.18	292.90	62.71	1.10	0.16	31.0	5.30	7.50
34	13.03.95	12.77	81.25	44.00	16.98	0.43	26.46	299.00	68.21	1.10	0.17	38.0	6.40	7.40
35	31.10.95	12.89	78.03	41.98	16.61	1.93	27.22	290.50	65.78	1.10	0.12	33.9	6.00	7.54

TABLE 7: Analytical results of major constituents in water from well 7 of the Jx.t reservoir (mg/l)

No.	Date	K	Na	Ca	Mg	Fe	Cl	HCO_3	SO_4	HBO_2	H_2S	SiO_2	F	pH
1	19.08.81	19.06	103.45	46.49	16.17	0.79	39.00	311.20	96.10	1.44	0.32	40.0	7.0	7.3
2	12.03.82	17.18	107.90	46.09	15.20	1.96	39.01	317.30	97.02	1.60	-	40.0	8.0	7.8
3	20.10.82	19.00	105.50	47.50	21.30	2.74	39.70	317.30	118.20	1.36	0.29	45.0	6.8	7.8
4	19.11.83	19.11	91.50	45.83	13.89	1.70	30.26	305.10	96.00	1.60	-	48.0	6.24	7.4
5	20.03.84	18.33	104.44	45.83	13.14	0.66	38.61	305.10	97.20	2.00	0.22	43.0	6.12	7.6
6	19.06.84	18.16	100.78	45.83	14.30	0.24	33.93	274.60	96.00	1.76	0.22	44.0	5.04	8.35
7	11.09.84	18.75	92.70	48.95	13.83	0.64	34.15	311.20	91.20	1.68	0.15	46.0	5.96	7.76
8	18.11.84	12.37	89.60	48.03	13.55	0.44	30.82	311.20	81.65	1.52	0.27	42.0	5.64	7.7
9	04.04.85	18.80	104.00	48.77	14.34	0.88	43.47	305.10	93.91	1.60	0.24	42.0	8.46	7.4
10	15.06.85	19.00	96.90	48.03	13.92	0.56	32.38	312.42	76.38	1.92	0.10	46.0	6.13	7.46
11	13.09.85	20.60	84.10	48.40	14.62	0.48	30.00	299.00	83.10	1.60	0.37	38.0	6.11	7.34
12	30.11.85	18.67	105.11	48.95	14.56	0.88	30.60	301.40	113.30	1.52	0.15	44.0	7.1	7.8
13	12.03.86	19.50	96.80	48.58	14.26	0.84	35.80	305.10	90.40	1.68	0.15	46.0	6.86	7.43
14	23.10.86	20.35	100.13	49.13	15.14	0.88	39.30	302.70	94.70	1.76	0.06	44.0	6.69	7.6
15	24.03.87	16.70	90.70	45.83	14.08	2.00	35.50	302.66	79.00	2.56	0.15	38.0	6.65	7.3
16	11.11.87	18.77	108.44	48.77	14.56	0.48	40.20	305.10	100.50	1.68	0.15	44.0	40.2	7.5
17	15.03.88	15.57	103.33	42.90	12.80	0.80	35.40	302.66	81.80	1.84	-	46.0	6.82	7.7
18	02.11.88	15.00	97.40	47.12	14.16	1.32	38.40	317.30	95.10	1.52	0.21	40.0	6.28	7.52
19	06.04.89	21.10	96.70	48.03	14.56	0.55	33.50	305.09	82.80	1.60	0.2	40.0	5.99	7.5
20	29.11.89	18.10	94.90	47.85	14.67	0.79	35.50	317.30	84.60	1.75	-	40.0	6.5	7.48
21	19.03.90	18.70	103.80	46.02	14.08	0.38	33.50	317.30	79.00	1.50	-	44.0	5.68	7.44
22	14.03.91	16.70	94.90	42.35	13.05	0.32	30.20	305.09	70.60	2.00	-	38.0	6.50	7.86
23	06.11.91	17.70	93.10	47.12	14.41	0.48	38.00	311.19	87.10	2.00	0.1	40.06	6.50	7.65
24	21.03.92	16.70	94.40	46.02	14.59	0.73	33.60	305.08	38.00	1.80	0.09	38.0	6.30	7.48
25	26.11.93	15.47	90.38	46.57	14.74	0.63	35.75	311.19	79.55	2.00	0.02	46.0	6.60	7.42
26	8.4.94	16.76	92.11	45.10	13.37	0.84	33.94	299.00	85.59	2.00	0.10	46.4	6.30	7.37
27	8.12.94	19.03	100.20	46.93	15.58	1.80	33.94	299.00	85.59	1.80	0.04	44.0	7.00	7.37
28	15.3.95	16.28	95.24	42.90	14.23	0.72	31.16	299.00	76.32	1.55	0.08	42.0	6.40	7.68
29	31.10.95	17.43	97.81	45.28	15.33	1.79	38.35	311.20	86.25	1.85	0.30	43.8	6.10	7.79

TABLE 8: Analytical results of major constituents in water from well 9 of the Cambrian system (mg/l)

No.	Date	K	Na	Ca	Mg	Fe	Cl	HCO_3	SO_4	HBO_2	H_2S	SiO_2	F	pH
1	04.11.83	17.20	84.9	51.33	15.4	2.0	28.1	286.80	98.0	0.12	-	25.0	6.04	8.00
2	20.03.84	14.67	88.89	45.83	14.97	1.68	20.78	286.80	105.3	0.80	-	26.0	5.76	7.74
3	22.06.84	13.67	82.22	47.67	15.40	1.13	17.40	289.00	88.80	0.72	-	24.0	4.68	7.82
4	10.09.84	14.38	72.70	47.30	14.91	1.76	17.54	270.90	98.40	1.04	-	27.0	5.58	8.21
5	13.06.85	14.88	79.10	41.48	14.91	1.12	16.51	283.13	91.30	1.36	0.59	28.0	5.74	7.92
6	13.09.85	16.10	68.90	50.23	15.53	2,54	17.00	278.20	93.70	0.80	-	24.0	6.40	7.46
7	12.03.86	15.70	79.00	50.97	15.47	1.18	19.20	280.70	93.30	0.96	-	29.0	6.15	7.61
8	23.10.86	16.07	79.86	50.42	16.24	1.31	20.70	286.80	96.30	1.12	-	27.0	6.21	7.60
9	24.03.87	14.87	87.11	49.50	16.02	1.60	19.80	286.79	97.50	1.84	0.07	27.0	6.55	7.85
10	14.10.87	14.07	84.89	49.32	15.60	1.50	21.60	290.46	100.00	0.96	0.20	28.0	6.06	7.40
11	15.03.88	14.60	83.78	50.05	15.55	0.96	20.80	292.90	106.40	1.60	-	28.0	5.78	7.30
12	02.11.88	11.90	75.80	50.97	15.63	3.50	20.00	297.78	100.6	0.96	0.04	25.0	5.76	7.70
13	06.04.89	17.30	81.30	50.05	15.33	0.12	19.30	286.79	90.60	0.88	-	23.0	5.56	7.57
14	29.11.89	13.10	78.10	49.50	15.88	0.92	21.60	292.89	89.10	1.00	-	25.0	6.00	7.56
15	17.03.90	16.60	78.80	51.52	15.55	0.17	21.30	280.69	93.70	1.00	-	30.0	5.93	7.48
16	19.11.90	16.00	79.70	48.22	15.95	0.76	20.40	298.99	91.70	0.88	0.06	27.0	6.20	7.72
17	13.03.91	15.50	81.30	48.95	15.66	0.60	22.00	292.89	89.40	2.00	-	28.00	6.00	7.64
18	22.10.91	14.00	72.90	49.68	16.10	2.50	21.70	286.78	85.70	1.00	0.07	30.00	6.10	7.70
19	19.03.92	13.80	75.60	48.22	15.66	3.49	21.90	286.78	85.30	1.20	-	24.0	5.70	7.84
20	17.11.92	11.62	74.60	49.48	15.97	4.04	21.90	292.88	84.50	1.40	0.27	22.0	6.20	7.60
21	16.03.93	14.30	77.77	48.77	15.25	2.10	20.10	286.78	91.60	1.50	-	24.0	6.00	7.66
22	05.11.94	15.08	75.38	49.32	15.84	1.55	21.16	283.10	85.32	1.00	0.22	26.0	6.20	7.71
23	13.03.95	15.15	77.26	46.93	16.17	2.20	21.45	268.50	90.55	1.15	0.12	28.0	6.20	8.05
24	31.10.95	14.79	78.91	48.03	16.39	4.56	23.12	274.60	89.14	1.00	0.08	28.6	5.90	8.04

TABLE 9: Analytical results of major constituents in water from different wells (mg/l)

Well No.	Date	K	Na	Ca	Mg	Fe	Cl	HCO_3	SO_4	HBO_2	H_2S	SiO_2	F	pH
1	05.04.89	13.90	76.7	44.0	15.73	0.4	25.3	292.89	65.70	1.12	0.07	30.0	5.81	7.22
4	05.04.89	19.00	85.6	49.87	14.22	0.401	27.2	311.20	78.00	1.00	0.00	35.0	6.00	7.72
5	05.04.89	18.50	84.40	50.42	14.26	0.25	29.70	311.20	77.60	1.20	-	30.0	6.19	7.22
7	06.04.89	21.10	96.70	48.03	14.56	0.55	33.50	305.90	82.80	1.60	0.20	40.0	5.99	7.50
8	06.04.89	19.00	100.00	51.33	15.03	0.34	30.30	317.30	97.50	1.20	0.07	35.0	5.56	7.25
9	06.04.89	17.30	81.30	50.05	15.33	0.12	19.30	286.79	90.60	0.88	-	23.0	5.56	7.57
11	11.04.89	18.00	88.10	40.88	14.67	1.12	29.40	286.79	70.20	1.40	0.13	40.0	6.11	7.35
16	18.6.91	12.90	74.80	48.95	15.14	1.24	21.30	292.88	92.60	1.08	-	29.0	6.00	7.73
30	11.03.96	3.27	94.82	46.75	20.17	2.00	61.46	299.00	74.88	2.00	-	59.8	6.60	7.03
32	28.10.94	4.70	68.02	37.07	20.67	1.84	20.24	274.60	54.80	0.82	-	27.0	6.40	7.34
35	29.06.95	9.91	77.85	39.23	17.53	0.31	33.40	262.40	62.10	1.00	0.28	39.1	7.20	7.78

5. CHEMICAL CHARACTERISTICS OF THE THERMAL FLUID

5.1 Stable isotopes

The stable isotopes of hydrogen and oxygen in natural waters were studied by Craig (1961a; 1961b). When natural water is evaporated in a system where thermodynamic equilibrium is maintained, the concentration of the components in the vapour and liquid phases are controlled by the respective vapour pressure. Experimental studies have shown that the isotopic relationship in meteoric water is governed by the natural water cycle of evaporation-condensation under equilibrium conditions. The oceanic precipitation is progressively depleted in the heavy isotopes as a function of distance of the precipitation from the local atmospheric reservoir. Two facts were observed. First, there will be an approximately constant ratio of $\delta D/\delta^{18}O$, indicating depletion relative to a given standard. Therefore, water derived from the meteorological cycle has a natural label and can be distinguished from any water derived from a source with a different isotopic relationship. This may provide a method of detecting juvenile components. Secondly, there is a general decrease in the heavy isotopic concentration as the latitude varies from equatorial to polar. This reflects a continuous loss of vapour from the air masses moving poleward. Consequently, precipitation has a latitude effect which is often complex and dependent on local meteorological conditions, hence, there are substantial time variations in the heavy isotopic concentrations of local precipitation.

The fact that precipitation is labelled by its isotopic concentration suggests an application along two lines. First, the ratio $\delta D/\delta^{18}O$ in thermal water indicates any admixtures with components that are not derived from oceanic-meteorological systems. Secondly, as thermal fluid and groundwater, in general, may percolate a long distance underground, their isotopic concentration may differ from that of local precipitation at the spring. Hence, a systematic study of the precipitation in the region may lead to the detection of a recharge area. This method is applicable both to groundwater hydrology and geothermal work. When oxygen isotopes are exchanged between hot rock and the circulating water, it is called oxygen shift. The extent of the oxygen isotope shift depends on the interaction temperature, water-rock ratio, interaction time and permeability of the rock. Generally, low temperature, high water-rock ratio and low interaction time result in a low oxygen isotope shift. Oxgyen shift may also be due to the presence of "andesite water" (Giggenbach 1992).

Figure 5 shows the δD and $\delta^{18}O$ relationship in thermal fluid and cold water from the Xiaotangshan geothermal field and other thermal fluids in the Beijing district. The data points concentrate along the meteoric line of Craig (1961a), demonstrating the meteoric origin of the thermal fluid. No $\delta^{18}O$ shift is observed due to low temperature of the geothermal reservoir. Because of lack of data, the seepage area cannot be determined.

5.2 Age of the thermal fluid

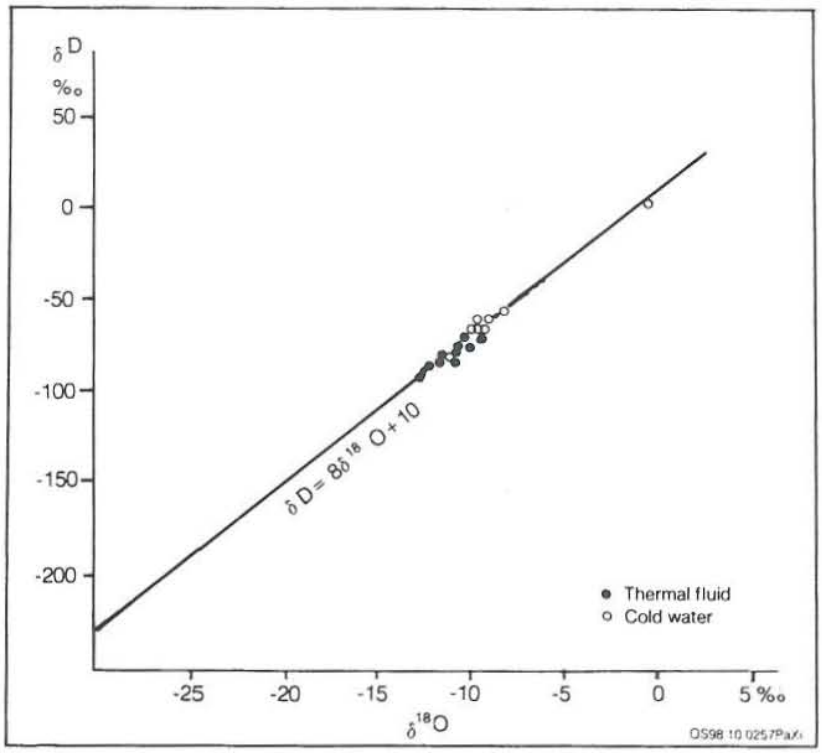

FIGURE 5: δD vs. $\delta^{18}O$ for geothermal and cold waters in the Beijing district

Libby (1949) suggested the use of radioactive ^{14}C as a dating method. The method can date carbon-containing material from the last 50,000-60,000 years. In general, carbon in groundwater can be derived from several different sources such as atmospheric CO_2, soil CO_2 of organic origin, CO_2 leached from rocks and from magmatic sources in volcanic areas. Generally, solvable inorganic carbon in groundwater is isolated from the atmosphere and soil-zone CO_2 and no longer interacts with ^{14}C from the outside. Age based on the ^{14}C method, therefore, shows time since groundwater became isolated from the atmosphere and the soil-zone. However, the age determination of groundwater with the method is rather complex due to the various origin of carbon in groundwater. Therefore the interpretation of ^{14}C determinations are often unclear and relative ages can be determined with more accuracy than absolute ages (Sveinbjörnsdóttir et al., 1995).

Groundwater age must increase along a flow path, or be an average age between the ages of two initial waters that mix. The age of mixed water has to increase along a flow path; thus the mixture has to be older than the youngest mixing water, and the final water may be older than both mixing waters at present, if travel times after mixing are long.

Five ^{14}C samples from the three reservoirs, two from Jx.w, one from Jx.t and two from the Cambrian system show that the age of the thermal fluid ranges between 24,000 and 30,000 years. The age of the fluid from well 1 is 24,000 years and from well 16 is 30,000, years indicating an increasing age of the thermal water from north to south. This is in agreement with other data which suggests that mixing of thermal fluids take place in the northern part of the field and a general flow direction is from north to south.

5.3 Classification of the thermal fluid

5.3.1 Cl-SO_4-HCO_3 triangular diagram

For the classification of thermal water a triangular plot of the three major anions, Cl-SO_4-HCO_3, is commonly used. The diagram indicates several types of thermal water such as immature waters, peripheral waters and volcanic and steam-heated waters. The diagram may provide some initial indication of a mixing relationship or geographic groupings, with e.g. Cl waters forming a central core grading into HCO_3 waters towards the margins of a thermal area. High SO_4 steam-heated waters are usually encountered over the more elevated parts of a field. The degree of separation between data points for high chloride and bicarbonate waters gives an idea of the relative degrees of interaction of the

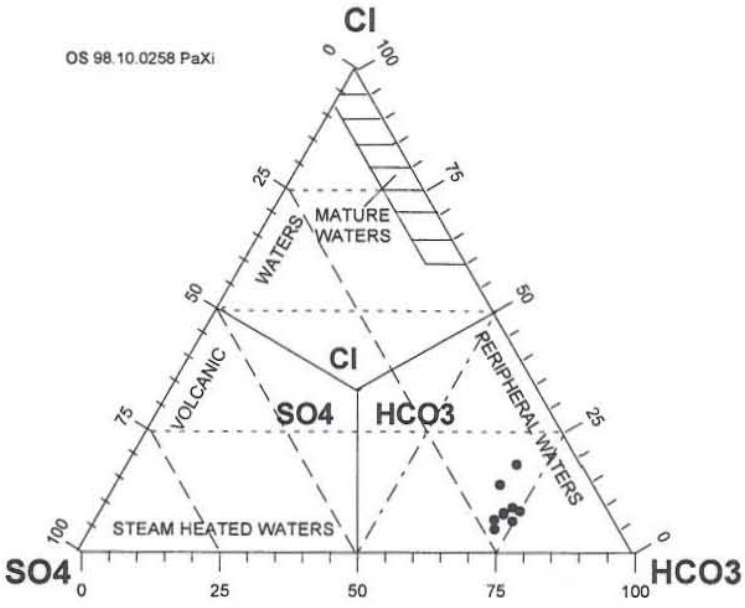

FIGURE 6: The Cl-SO_4-Mg triangular diagram for the Xiaotangshan waters

CO_2 charged fluids at lower temperature, and of the HCO_3 contents increasing with time and distance travelled underground.

The triangular diagram also allows the weeding out of unsuitable waters. Most geochemical techniques are not applicable to acidic waters. The group best suited comprises the neutral, low sulfate, high chloride geothermal waters along the Cl-HCO_3 axis, close to the Cl corner. In the case of albeit neutral, but high bicarbonate waters, considerable caution is required in the application of most "geoindicators".

The position of a data point is simply obtained by first forming the sum S of the concentrations C (in mg/l) of all three constituents involved (Giggenbach, 1991),

$$S = C_{Cl} + C_{SO4} + C_{HCO3}$$

and then by calculating the %-Cl, %-HCO_3 and %-SO_4.

Figure 6 shows that all data points from the three reservoirs plot close to the HCO_3 corner indicating that the thermal fluid belongs to peripheral waters.

5.3.2 Na-K-Mg triangular diagram

Giggenbach (1988) suggested that a triangular diagram with Na/1000, K/100, and $\sqrt{Mg}$ at the apices can be used to classify waters into full equilibrium, partial equilibrium and immature waters (dissolution of rock with little or no chemical equilibrium). The triangular diagram is employed to determine whether the fluid has equilibrated with hydrothermal minerals as well as to predict the equilibration temperatures, $T_{Na\text{-}K}$ and $T_{K\text{-}Mg}$. The Na-K-Mg triangular diagram provides an indication as to the suitability of a given water for the application of ionic solute geoindicators. It is based on the temperature dependency of the full equilibrium assemblage of potassium and sodium minerals that are expected to form after isochemical recrystallization of average crustal rock under conditions of geothermal interest. The use of the triangular diagram is based on the temperature dependence of the three reactions:

$$K\text{-}feldspar + Na^+ = Na\text{-}feldspar + K^+$$

$$0.8\,muscovite + 0.2\,clinochlore + 5.4\,silica + 2Na^+ = 2\,albite + 0.8\,K\text{-}feldspar + 1.6\,water + Mg^{2+}$$

$$0.8\,muscovite + 0.2\,clinochlore + 5.4\,silica + 2K^+ = 2\,albite + 2\,albite + 2.8\,K\text{-}feldspar + 1.6\,water + Mg^{2+}$$

Figure 7 shows that all the data points plot in the area of immature waters, very close to the $\sqrt{Mg}$ corner of the diagram, which may indicate that the thermal fluid is a mixture of cold groundwater. Based on the diagram, it is not possible to use K-Na and K-Mg geothermometers to estimate reservoir and discharge temperatures for the thermal fluid of the Xiaotangshang geothermal field.

5.4 The thermal fluid mixing and recharge area

Mixing of two waters can be indicated on a plot of one conservative species against another. Figure 8 shows that the relationships of Cl-B, Cl-K, Cl-Na and Cl-Ca are close to a linear relationship. Arnórsson (1985) suggested that such a linear relationship is evidence of mixing. Truesdell (1991) suggested using the Schoeller diagram as an introduction to the water chemistry of a geothermal area and as an effective tool for showing the mixing of different waters. Figure 9 shows that the contents of Na and HCO_3 in cold water are similar to that in thermal fluid, but the contents of Fe, K, F and HBO_2 in cold water are much lower than that in thermal fluid. K, Fe and HBO_2 concentrations show that almost all thermal fluids have some cold water admixed, but the quantity is not so much for changes in Mg, Ca, and F to be obvious in the Schoeller diagram. The diagram proves that there is some mixing of cold water from the field or the neighbouring area, but its mixing quantity is not high. The conclusion is in accordance with the formation structure in the field. The bottom of the Quaternary formation is fine clay which is an aquiclude, and all geothermal wells are cased in all of the Quaternary formation. The thermal fluid cannot mix with a large quantity of cold water from the field and neighbouring area. The thermal fluid is recharged mainly by cold water from groundwater runoff. The following evidence supports this:

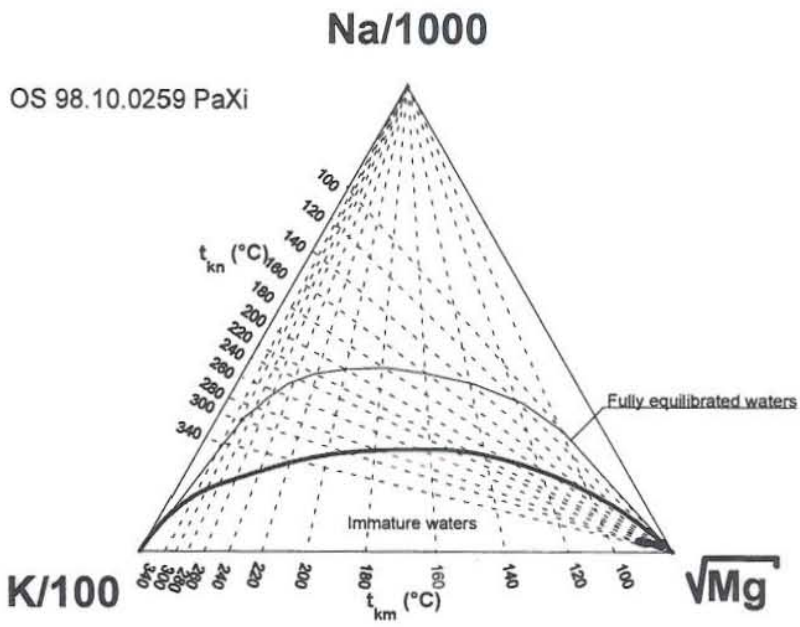

FIGURE 7: The Na-K-Mg triangular diagram for the Xiaotangshan waters

1. The ^{14}C dating data shows that the thermal fluid is recharged by cold water from groundwater runoff and its recharge area is located to the north of the field.
2. On the triangular diagrams, Cl-SO_4-HCO_3 and Na-K-Mg, all samples from the three reservoirs, plot close to each other in the field of peripheral water and immature waters, respectively. This can be explained by the mixing of hot and cold waters.
3. Discharge temperature of waters from well 1 located in the northern part of the field decreased from 53.5°C in 1974 to 51°C in 1995, on the other hand discharge temperature of waters in the middle and southern part of the geothermal field has changed very little. It is a good evidence that the thermal fluid is mixed with cold water which comes mainly from groundwater runoff, and that the feed area is in the northern part of the field.

5.5 WATCH program and equilibrium calculation for selected wells

The computer program WATCH (Arnórsson et al.,1982; 1983; Bjarnason, 1994) was used to calculate the reservoir temperature and the saturation index of several minerals. The computation consists of the following steps:

1. Ionic strength and ionic balance found according to analysed chemical compositions of water sampled at well head;
2. Calculating the corresponding concentration of each chemical composition in deep water;
3. Determining the activity coefficients of every species in deep water;
4. The chemical components in deep water;
5. Ionic strength and ionic balance measured in deep water;

6. The standard chemical geothermometers used;
7. Finally, the logarithm of solubility products of 29 geothermal minerals in deep water are shown.

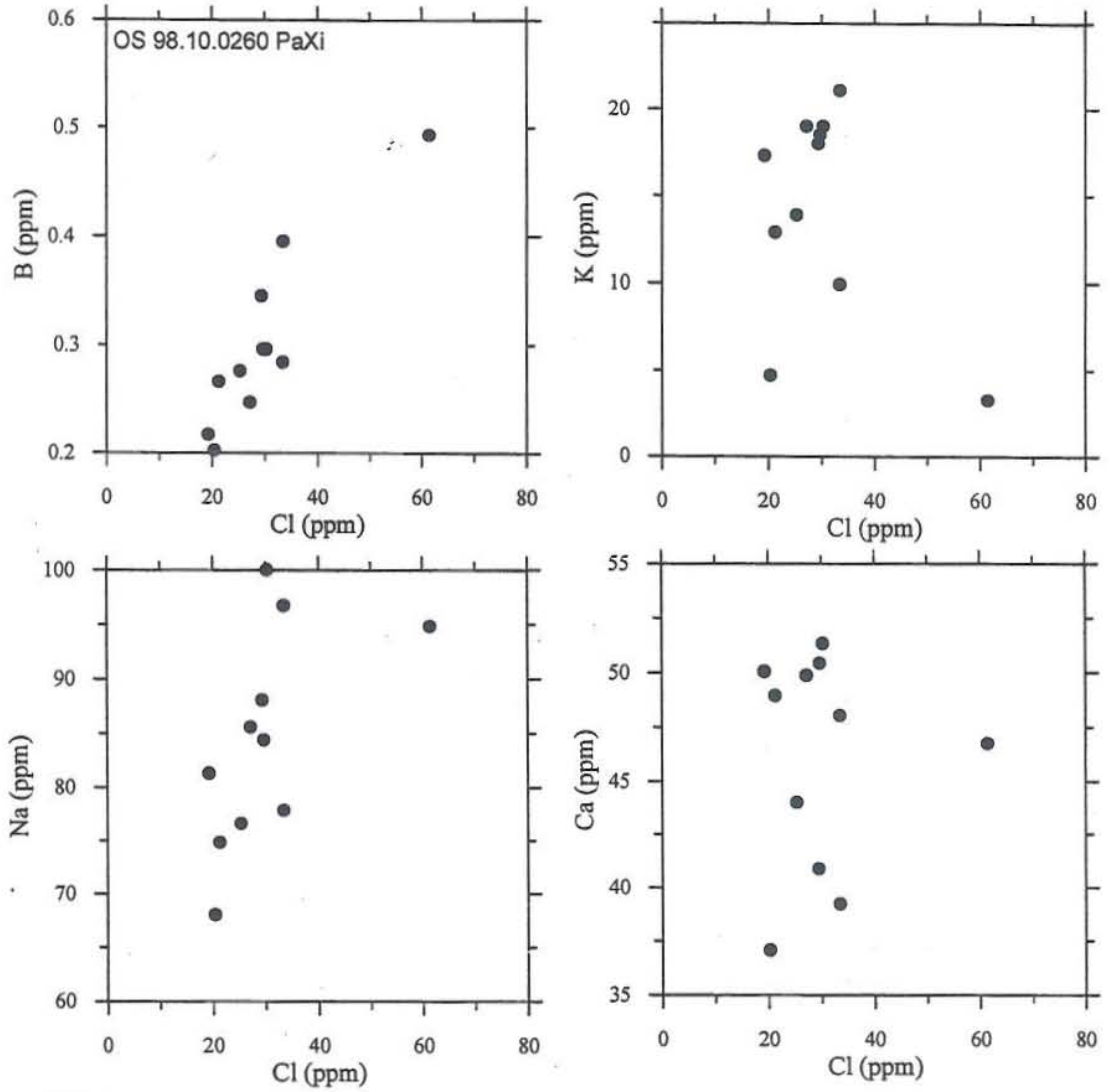

FIGURE 8: Relationship of Cl vs. B, K, Na, and Ca in thermal waters in Xiaotangshan

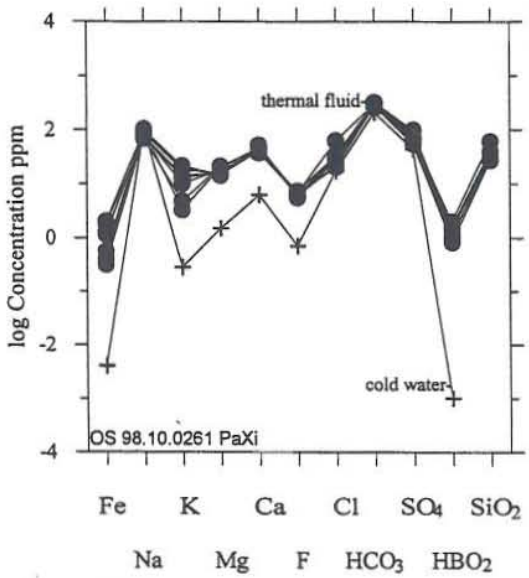

FIGURE 9: Schoeller diagram for thermal and cold waters in Xiaotangshan

If the calculated value of a mineral is equal to its theoretic value (log(Q/K) = 0), the mineral has reached equilibrium with the water in the reservoir. If a group of minerals is close to equilibrium at one particular temperature, it means that the water has equilibrated with this group of minerals and the temperature represents the reservoir temperature.

Several samples from one spring and selected wells from the three reservoirs were chosen for equilibrium calculations with the WATCH program. For reservoir formation Jx.w, a spring and well 30 were chosen, for the Jx.t reservoir wells 4 and 7 were chosen, and for the Cambrian system wells 8 and 9 were chosen. The results are shown in Figure 10. It indicates that there is no clear thermal water-rock equilibrium at one particular temperature. Because of low temperature and mixing, the thermal fluid is not in equilibrium with hydrothermal minerals, except for chalcedony which is near equilibrium close to discharge temperature in almost all samples.

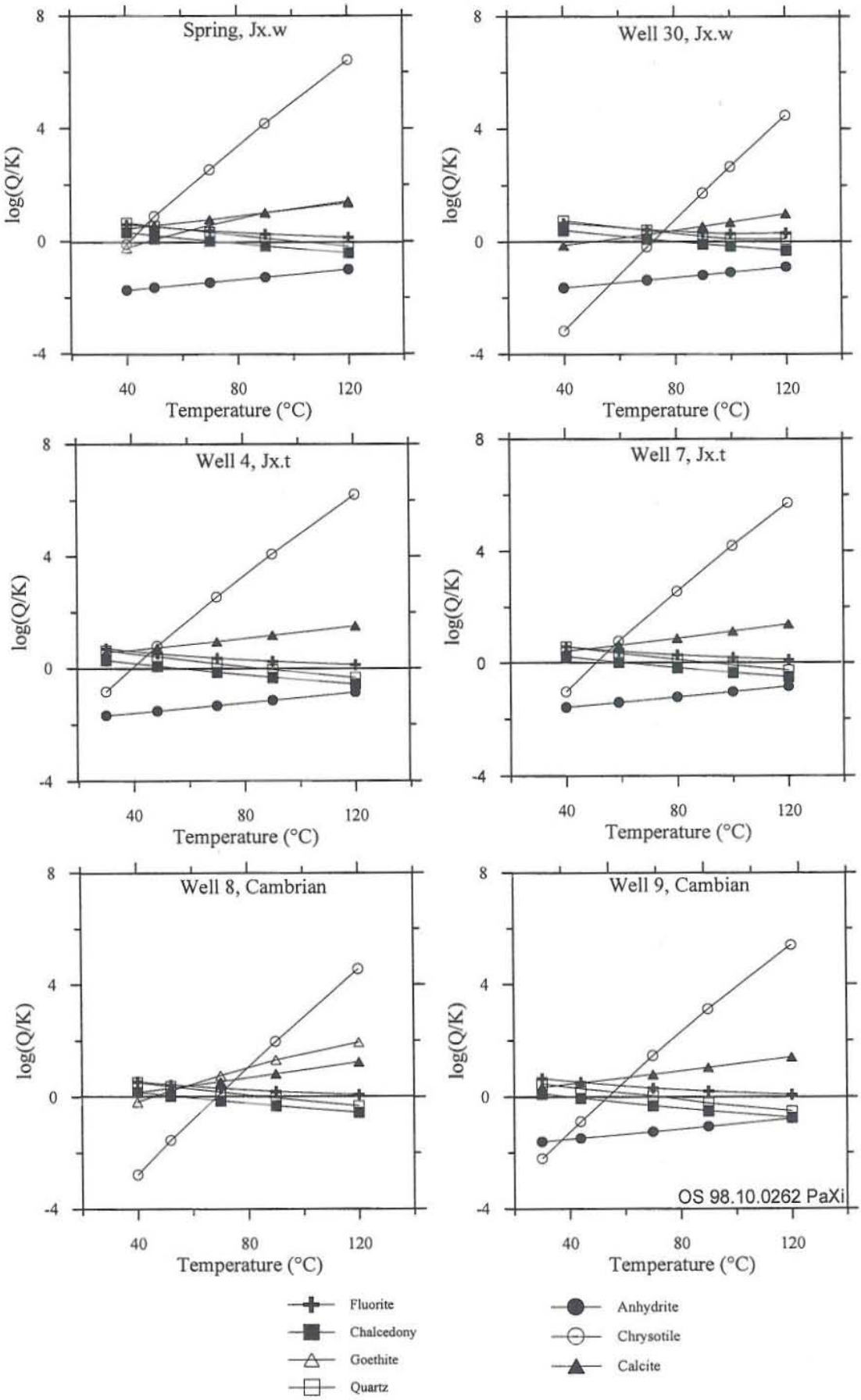

FIGURE 10: The log (Q/K) diagrams for selected Xiaotangshan samples

5.6 Geothermometers

One of the major applications of geochemistry in the investigation of geothermal resources involves prediction of subsurface temperature using chemical geothermometers. Geothermometers may be broadly classified into two groups : (1) Those which are based on temperature-dependent variations in solubility of individual minerals, and (2) those which are based on temperature-dependent exchange reactions which fix ratios of certain dissolved constituents. Within group (1) the silica minerals are ideal for geothermometry (Fournier, 1991).

5.6.1 Silica geothermometers

The solubilities of all silica minerals decrease drastically as temperature decreases below 340°C. At high temperature the silica geothermometers can be used with the assumptions, that the thermal fluid is in equilibrium with quartz in the reservoir, the pore fluid pressure in the reservoir is fixed by the vapour pressure of pure water, there is no mixing of hot and cold waters during upflow, and there is either conductive cooling of the ascending water or adiabatic cooling with steam separation at 100°C.

The solubility of quartz appears to control dissolved silica in geothermal reservoirs at temperatures higher than 120-180°C. There is an ambiguity in the use of silica geothermometers at temperatures less than about 180°C, because chalcedony appears to control dissolved silica in some places and quartz in others. Chalcedony is a very fine-grained variety of quartz composed of aggregates of very tiny crystals. The individual quartz grains are so small that they have relatively large surface energies compared to "normal" quartz, and this results in increased solubility. Chalcedony is unstable in contact with water at temperatures above 120-180°C, because the smallest sized crystals completely dissolve relatively quickly, and large sized crystals grow large enough so that surface energy is no longer a factor. Temperature, time, fluid composition, and prior history all affect the size attained by quartz crystals. Thus, in some places where water has been in contact with rock at a given temperature for a relatively long time, such as in some deep sedimentary basins, quartz may control dissolved silica even at temperatures less than 100°C. In other places, chalcedony may control dissolved silica at temperatures as high as 180°C (particularly in newly fractured portions of hydrothermal systems).

The quartz geothermometer of Fournier (1977) for quartz with no steam loss (SiO_2 in mg/l) is given as

$$t(°C) = \frac{1032}{4.69 - \log SiO_2} - 273.15$$

and the chalcedony geothermometer (SiO_2 in mg/l) of Fournier (1973) as

$$t(°C) = \frac{1309}{5.19 - \log SiO_2} - 273.15$$

Quarts and chalcedony temperatures have been calculated for thermal waters from selected wells of the Xiaotangshan geothermal field. The results are shown in Table 10.

Chalcedony geothermometer temperatures vary from 37 to 81°C. Quartz geothermometer temperatures vary from 68 to 110°C and are obviously higher than discharge and chalcedony geothermometer temperatures. Quartz geothermometer temperatures may reflect deep reservoir temperatures near the thermal resource. Chalcedony geothermometer temperatures are equal or close to discharge temperatures. But the chalcedony temperature of wells 35 and 40 are below the discharge temperature by 10 and 15°C respectively. This could indicate that the thermal water in wells 35 and 40 could be

TABLE 10: Discharge and geothermometer temperatures

Well no.	SiO_2	$T_{meas.}$ (°C)	$T_{Chalcedony}$ (°C)	T_{Quartz} (°C)
Spring	49	51	71	101
Artesian	44.2	51	66	96
Well 1	37.5	53.5	58	89
Well 4	35	48.5	55	86
Well 7	40	60	61	92
Well 8	35	52.5	55	86
Well 9	23	44	37	69
Well 11	40	64.5	61	92
Well 20	33	50.5	52	83
Well 30	59.79	70	81	110
Well 35	39.14	70	60	91
Well 40	25.22	56	41	72

mixing with cold water coming from drilling. Chalcedony geothermometer temperatures are higher than artesian and spring temperatures by about 15-20°C.

The results of the WATCH calculations show that chalcedony is in equilibrium in all samples at temperatures close to the discharge temperatures. The results of geothermometer calculation as well as the data on thermal fluid-rock equilibrium prove that chalcedony geothermometers are more suitable than the quartz geothermometer to estimate reservoir temperatures in the Xiaotangshan geothermal field. Chalcedony controls dissolved silica in the reservoirs of the field. The Chalcedony geothermometer temperature of well 30, which is located in the eastern part of the field, is 81°C, higher than any measured temperature within the geothermal field. It indicates that it may be possible to get thermal fluid with discharge temperature of about 80°C close to well 30, so there is potential for developing the geothermal resources in the eastern part of the field.

5.6.2 Cation geothermometers

Cation geothermometers are also widely used to estimate subsurface temperatures. They are based on ion exchange reactions with temperature dependent equilibrium constants. There are different cation geothermometers. The Na-K geothermometer is based on the exchange of Na^+ and K^+ ions between coexisting alkali feldspars with temperature-dependent equilibrium

$$NaAlSi_3O + K^+ = KAlSi_3O_8 + Na^+$$

The Na-K geothermometer (Na and K in mg/l) of Fournier (1979) is given as

$$t(°C) = \frac{1217}{1.483 + \log(Na/K)} - 273.15$$

The K-Mg geothermometer (Giggenbach, 1988) based on the equilibrium between water and the mineral assemblage K-feldspar, K-mica and chloride, is found to respond to changes in the physical environment and usually gives a relatively low temperature. The geothermometer is suitable for low-temperature reservoir. It is based on the temperature dependence of the following reaction:

$$2.8K\text{-}feldspar + 1.6water + Mg^{2+} = 0.8K\text{-}mica + 0.2chloride + 5.4silica + 2K^{+}$$

K-Mg geothermometer (K and Mg in mg/l) of Giggenbach (1988) is given as

$$t(°C) = \frac{4410}{14.0 - \log(K^2/Mg)} - 273.15$$

As pointed out in Figure 7, the thermal fluids of the Xiaotangshang geothermal field are immature waters, and therefore the cation geothermomters cannot be applied. However, temperatures based on the Na-K and K-Mg geothermometers were calculated. The former were found to range from 140 to 296°C, far too high to be reasonable for the geothermal system, whereas temperatures based on the K-Mg geothermometer range from 35 to 79°C, much closer to discharge and chalcedony temperatures. Therefore, the Na-K temperatures were not used at all for this interpretation, but the K-Mg temperatures were used to indicate a trend in the change of reservoir temperature.

6. WATER LEVEL, CHEMICAL AND TEMPERATURE CHANGES DURING UTILIZATION

6.1 Water level changes

The water level is inversely proportional to the amount of water exploited from the geothermal system. When exploitation increases, water level drops. The relationship between water level and exploited yield is shown in Figure 11 for Jx.w reservoir (A) and Jx.t reservoir (B). For the winter space heating season from November to April, extraction increases and the water level lowers. During June to October, extraction decreases and water level rises again. Annual lowest water levels appear in February. The highest water level appears in September. Water level has decreased at approximately the same rate for all three reservoirs during the period 1987-1995 (Pan, 1996).

6.2 Chemical changes

Three wells have been used for chemical monitoring of the geothermal field, well 1 for the Jx.t reservoir from 1974 to 1995, well 7 for the Jx.t reservoir from 1981 to 1995 and well 9 for the Cambrian reservoir from 1983 to 1995. The chemical concentration of the 8 main components of the thermal water from each well are shown plotted against time in Figures 12 and 13. The components are potassium (K), sodium (Na), calcium (Ca), and magnesium (Mg), in Figure 12 and chloride (Cl), bicarbonate (HCO_3), silica (SiO_2) and sulphate (SO_4) in Figure 13. The main observations based on Figures 12 and 13 are as follows:

Potassium: The concentration of potassium (K) in water from the three wells ranges approximately from 10 to 20 ppm, and there is no indication that the concentration has changed during the monitoring period.
Sodium: The concentration of sodium (Na) ranges from approximately 70 to 110 ppm. The concentration has been relatively stable in all wells, except it decreased in well 1 from 1980 to1987.
Magnesium: The concentration of magnesium (Mg) ranges from 12 to 22 ppm and no significant change has taken place in water from the wells. Three samples with unusually high magnesium concentrations, two from well 1 and one from well 7, are unexplained.
Chloride: The concentration of chloride (Cl) in the three wells ranges from approximately 15 to 45 ppm. No changes have been observed in water from wells 7 and 9. The Cl concentration decreased in water from well 1 from 1973 to 1986, but has been stable since.
Bicarbonate: The bicarbonate (HCO_3) concentration ranges from approximately 270 to 320 ppm. One sample from well 1 shows an unusually low value of approximately 245 ppm in 1986. No clear correlation is obvious between the concentration of bicarbonate and time in any of the wells.

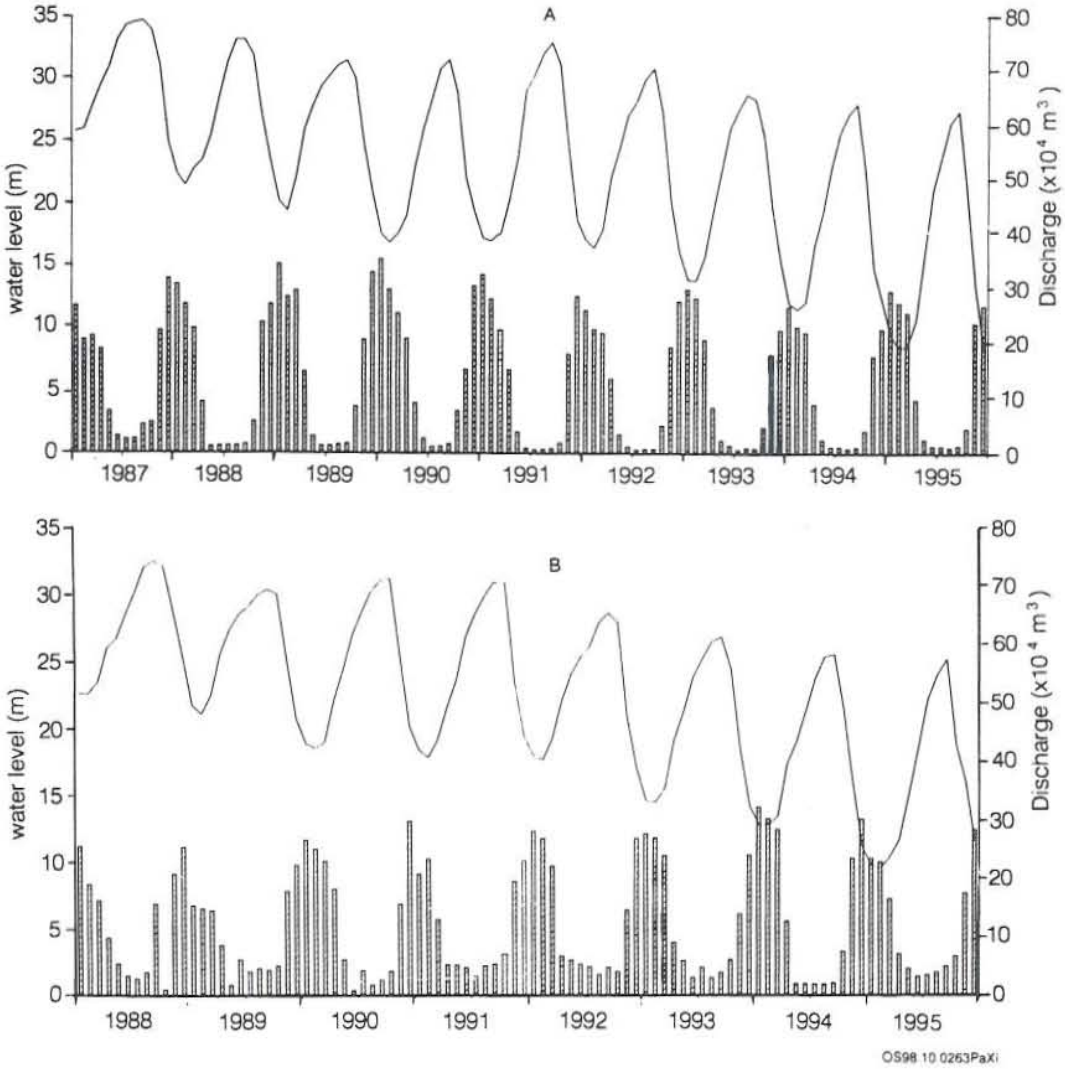

FIGURE 11: Water level changes and production from the Xiaotangshan field for the period 1988-1995

Silica: The silica (SiO_2) concentration in the three wells ranges from approximately 20 to 60 ppm, and the concentration has been stable in wells 7 and 9. In well 1 the silica concentration decreased drastically from 1973 to 1983 but has been more or less stable since.

Sulphate: The sulphate (SO_4) concentration ranges from approximately 40 to 150 ppm. The concentration increased in well 1 from 1973 until 1976, but has since decreased in all three wells that are useful for monitoring.

The main features of the chemical changes are as follows:

1. The concentrations of some elements decreased quickly at first, then they changed very little or became stable, for example SiO_2, SO_4, Cl.
2. The concentrations of elements in waters from well 1 declined more and earlier than in waters from well 7 and well 9. For example, the SiO_2 concentration in well 1 water decreased from 58 mg/l to 33 mg/l, but was almost stable in water from wells 7 and 9. The Ca concentration decreased in well 1 from 1973, in well 7 from 1987 and in well 9 from 1990.

The chemical changes can be explained by changes in the thermal fluid exploited from the area. The concentrations of the main 8 elements in three reservoirs were stable or changed very slowly as exploitation yield was stable from 1987 to 1995. The chemical observations indicate that the thermal fluid is recharged by cold groundwater in the northern part of the field and the flow direction of the thermal fluid in the field is from north to south.

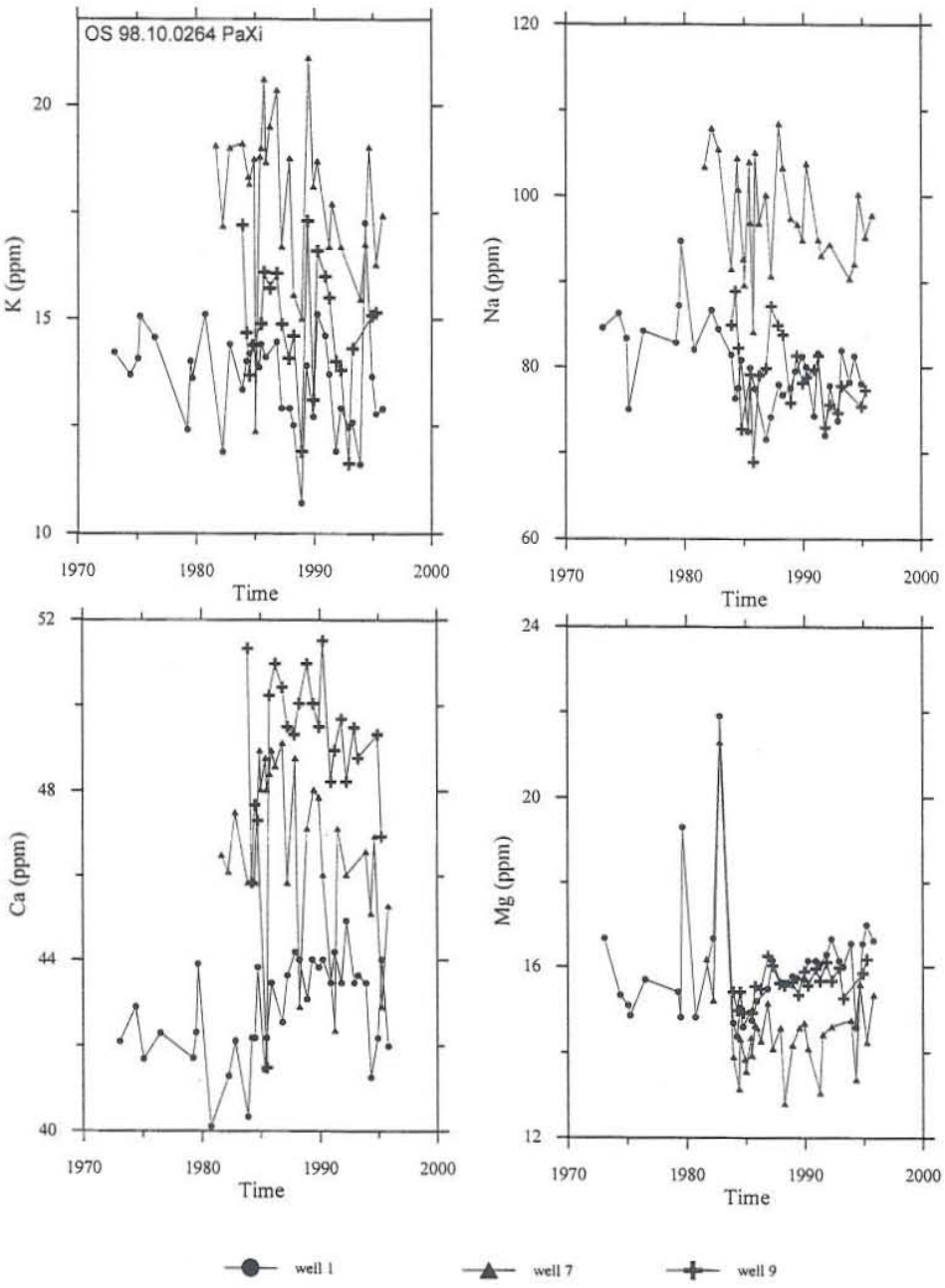

FIGURE 12: K, Na, Ca, and Mg changes with time for Xiaotangshan waters

6.3 Temperature changes

Discharge temperature of well 1 decreased from 53.5°C in 1974 to 51°C in 1995. There are a few wells in the northern part of the field where temperature decreased. The temperature decrease of well 1 is the largest of all wells. Discharge temperatures of wells in the middle and southern part of the field have not changed. Detailed temperature measurements at wellhead are scarce and can, therefore, not be used to study temperature changes during utilization. However, due to abundant chemical data, calculated temperatures based on geothermometers can be used to study past temperature changes and possible future changes during utilization.

Chalcedony, quartz and K-Mg geothermometers were selected to calculate temperatures of the three reservoirs. The results for samples from well 1 (1975 to 1995), well 7 (1981 to 1995) and well 9 (1983 to 1995) are shown in Table 11. A five year average temperature has been calculated for each well and is also shown in Table 11.

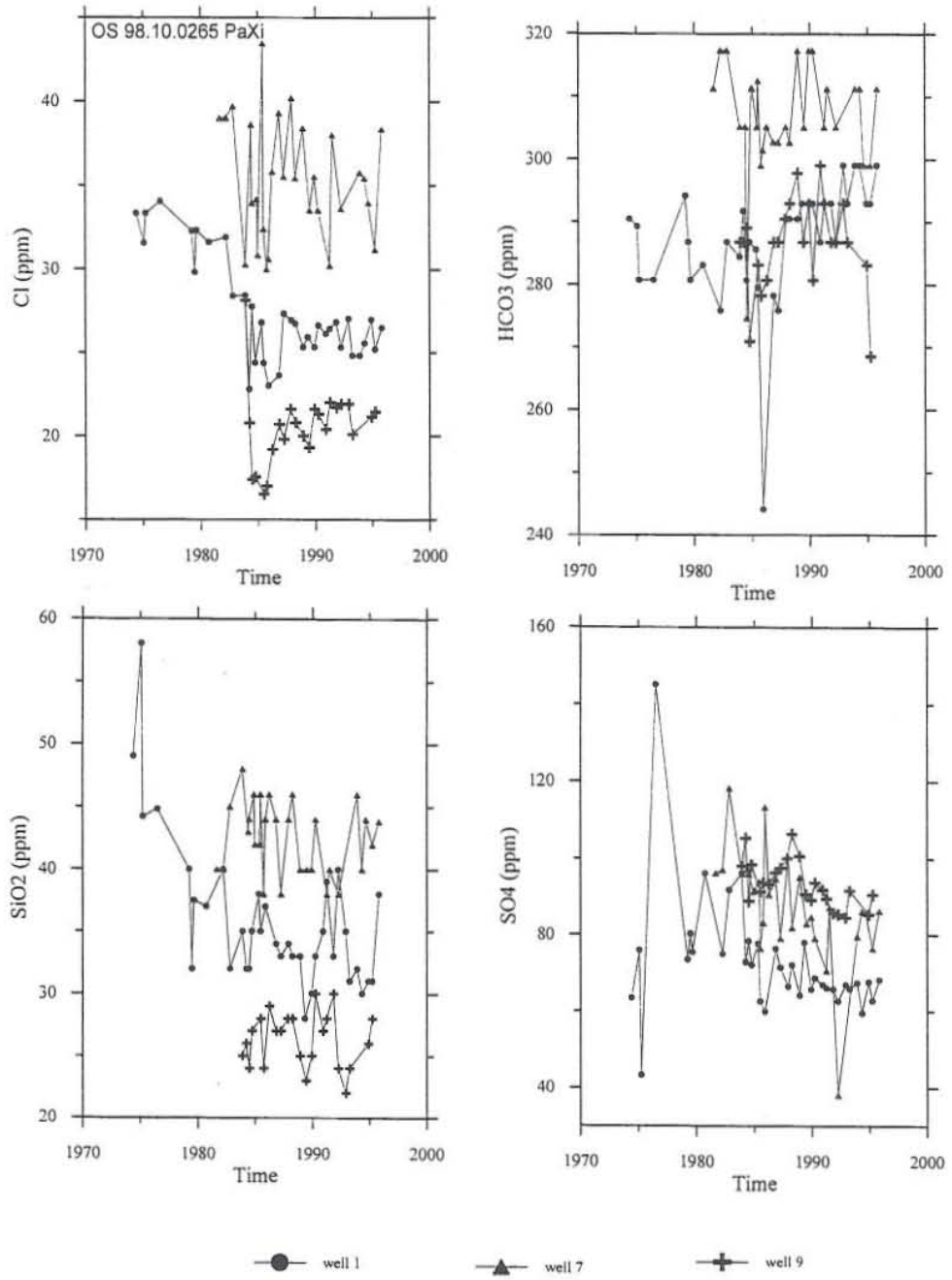

FIGURE 13: Cl, SiO_2, SO_4 and HCO_3 changes with time for Xiaotangshan waters

The main features of the temperature changes are:

1. **Well 1:** T_{ac} decreased 1975-1980 then stabilized; T_{aq} decreased 1975-1980 then stabilized; T_{aKMg} more or less stable 1975-1995.
2. **Well 7:** T_{ac} more or less stable 1981-1995, T_{aq} more or less stable 1981-1995, T_{aKMg} more or less stable 1981-1995.
3. **Well 9:** T_{ac} more or less stable 1983-1995, T_{aq} more or less stable 1983-1995, T_{aKMg} more or less stable 1983-1995.
4. The only significant decrease in temperature, based on geothermometer calculations, is in well 1. For the other wells, 7 and 9, geothermometer temperatures changed little. Geothermometer temperature changes coincide with changes in measured temperatures. This can indicate that it is possible to use geothermometers to reveal and forecast temperature changes in the reservoirs. The geothermometer temperature changes supply further evidence that the main recharge resource of the thermal fluid comes from cold groundwater to the north of the field and direction of the thermal fluid movement is from north to south.

TABLE 11: Three reservoir geothermometer temperatures (°C) in chemically monitored well waters

No.	Date	Tc	Tac	Tq	Taq	T_{K-Mg}	T_{aK-Mg}
Well 1, Jx.w, discharge temperature:53.5°C							
1	29.1.1975	65.8		96.1		69.2	
2	1.3.1975	66.5		96.8		70.2	
3	4.6.1976	61.1		91.7		69.6	
4	29.3.1979	50.9	60.1	82.1	90.8	68.8	69.2
5	11.6.1979	58.1		88.9		69.3	
6	18.8.1979	57.4		88.3		65.6	
7	24.9.1980	61.1		91.7		71.1	
8	12.3.1982	50.9		82.1		64.2	
9	20.10.1982	54.9		85.9		65.5	
10	4.11.1983	50.9		82.1		68.3	
11	14.3.1984	50.9		82.1		69.6	
12	21.6.1984	54.9	54.1	85.9	85.1	69.4	68.4
13	11.9.1984	58.7		89.4		70.1	
14	2.4.1985	54.9		85.9		69.0	
15	15.6.1985	57.4		88.3		70.0	
16	27.11.1985	53.6		84.6		69.2	
17	23.10.1986	52.2		83.4		69.5	
18	24.3.1987	53.6		84.6		66.4	
19	7.11.1987	52.2		83.4		66.8	
20	14.3.1988	52.2		83.4		66.1	
21	1.11.1988	45.1	52.3	76.6	83.4	62.5	67.3
22	5.4.1989	48.1		79.4		68.4	
23	22.11.1989	52.2		83.4		66.4	
24	19.3.1990	54.9		85.9		70.0	
25	20.11.1990	59.9		90.6		69.3	
26	14.3.1991	52.2		83.4		67.9	
27	22.10.1991	61.1		91.7		64.5	
28	16.3.1992	54.9		85.9		66.1	
29	19.11.1992	49.5		80.8		65.6	
30	16.3.1993	50.9		82.1		65.9	
31	26.11.1993	48.1	52.8	79.4	83.9	63.8	66.7
32	8.4.1994	49.5		80.8		74.4	
33	5.11.1994	49.5		80.8		67.4	
34	13.3.1995	58.7		89.4		65.6	
35	31.10.1995	53.4		84.5		66.1	
Well 7, Jx.t, discharge temperature: 59.5°C							
1	19.8.1981	61.1		91.7		75.5	
2	12.3.1982.	61.1		91.7		73.8	
3	20.10.1982	66.7		97.0		72.2	
4	19.11.1983	69.8		99.9		77.4	
5	20.3.1984	64.5		94.9		77.1	
6	19.6.1984	65.6		95.9		75.8	
7	11.9.1984	67.8		97.9		77.0	
8	18.11.1984	63.4		93.9		67.5	
9	15.6.1985	63.4		93.9		76.6	
10	15.6.1985	67.8		98.0		77.2	
11	13.9.1985	58.7	64.6	89.4	95.0	78.6	75.4
12	30.11.1986	65.6		95.9		76.3	
13	12.3.1986	67.8		97.9		77.6	
14	23.10.1986	65.6		95.9		77.9	
15	24.3.1987	58.7		89.4		74.0	
16	11.11.1987	65.6		95.9		76.4	
17	15.3.1988	67.7	63.6	98.0	94.0	73.5	75.7
18	2.11.1988	61.1		91.7		71.4	
19	6.4.1989	61.1		91.7		79.2	
20	29.11.1989	61.1		91.7		75.4	
21	19.3.1990	65.6		95.9		76.7	
22	14.3.1991	58.7		89.4		74.9	
23	6.11.1991	61.1		91.7		75.1	
24	21.3.1992	58.7		89.4		73.6	
25	26.11.1993	67.8	63.8	98.0	94.3	71.7	74.4
26	8.4.1994	68.2		98.4		74.7	
27	8.12.1994	65.6		95.9		75.9	
28	15.3.1995	63.4		93.9		73.3	
29	31.10.1995	65.4		95.7		74.0	
Well 9, Cambrian, discharge temperature: 44°C							
1	4.11.1983	40.3		72.0		73.6	
2	20.3.1984	42.0		73.6		70.2	
3	22.6.1984	38.7		70.4		68.3	
4	10.9.1984	43.5		75.1		69.8	
5	13.6.1984	45.1		76.6		70.6	
6	13.9.1985	38.7	42.7	70.4	74.3	72.0	70.6
7	12.3.1986	46.1		78.0		71.4	
8	23.10.1986	43.5		75.1		71.4	
9	24.3.1987	43.5		75.1		69.8	
10	14.10.1987	45.1		76.6		68.8	
11	15.3.1988	45.1		76.6		69.7	
12	2.11.1988	40.3		72.0		65.0	
13	6.4.1989	36.9		68.8		73.8	
14	29.11.1989	40.3		72.0		67.0	
15	17.3.1990	48.1		79.4		72.7	
16	19.11.1990	43.5	42.1	75.1	73.7	71.5	69.2
17	13.3.1991	45.1		76.6		71.0	
18	22.10.1991	48.1		79.4		68.3	
19	19.3.1992	38.7		70.4		68.3	
20	17.11.1992	35.1		67.1		64.2	
21	16.3.1993	38.7		70.4		69.4	
22	5.11.1994	42.0	42.9	73.6	74.5	70.2	69.8
23	13.3.1995	45.1		76.6		70.1	
24	31.10.1995	46.0		77.4		69.4	

Tc: Chalcedony geothermometer temperature; Tac: 5 y. average chalcedony geothermometer temp.;
Tq: quartz geothermometer temperature; Taq: 5 years average quartz geothermometer temp.;
T_{K-Mg}: K-Mg geothermometer temperature; T_{aK-Mg}: 5 years average K-Mg geothermometer temp..

7. CONCLUSIONS

The main objectives of the work were to study geochemical characteristics of thermal fluids from the Xiaotangshan geothermal field, to define mixing and the main origin of mixed water, to study and predict the changes in concentration of main compositions and subsurface temperature changes with time during utilization. The main conclusions are as follow:

1. Stable isotope δD and $\delta^{18}O$ relationship proves that the origin of the thermal fluid is meteoric.
2. Based on ^{14}C data the age of the thermal fluid is about 24,000-30,000 years.
3. The direction of the flow of the thermal fluid is from north to south as indicated by the data of age, temperature and chemical changes of the thermal fluid.
4. The thermal fluid belongs to peripheral waters and immature waters.
5. The thermal fluid is recharged by cold groundwater. The recharge zone is in the north of the field. Groundwater runoff is the main recharge source. There is a small amount of cold shallow groundwater from the field or neighbouring area mixing with the thermal fluid during upflow.
6. Because of low temperature and mixing, the thermal fluid is not in equilibrium with hydrothermal minerals.
7. The chalcedony geothermometer is suitable to estimate temperatures of the reservoirs in the field. It is possible from the results of the chalcedony geothermometer to obtain higher discharge temperature than 70°C which is the highest discharge temperature at present, and there is potential for developing geothermal resources in the eastern part of the field.
8. The SiO_2 ,Cl, SO_4, and Na concentrations from well 1 declined quickly with time before 1987, then became stable or decreased very slowly between 1987 and 1995. Chemical changes in wells 7 and 9 were smaller than in well 1.
9. Geothermometer temperatures for the reservoirs decreased with time before 1989, then were stable or even increased.
10. The features of the chemical and temperature changes with time indicate that the main chemical compositions of the thermal fluid and temperatures in three reservoirs will be stable or change very slowly if the field is exploited under the same conditions as between 1987 and 1995.

ACKNOWLEDGEMENTS

I would like to express my gratitude to Dr. Ingvar B. Fridleifsson and Mr. Lúdvík S. Georgsson for the UNU fellowship award and also for technical support, and to Ms. Gudrún Bjarnadóttir for her efficient help and cooperation during all the training. To my supervisor, Mr. Magnús Ólafsson, sincere thanks for patient guidance during all the stages of the preparation of this report and for allowing me to receive the benefits of his experience and knowledge. Thanks are due Dr. Jón Örn Bjarnason and Dr. Halldór Ármannsson for their valuable advice, beneficial discussions and help. My gratitude also goes to Dr. Stefán Arnórsson for two weeks of training in thermodynamics and his excellent lectures. I convey my good wishes to all other lecturers and the staff of Orkustofnun for sharing their knowledge and help.

REFERENCES

Arnórsson, S., 1985: The use of mixing models and chemical geothermometers for estimating underground temperature in geothermal systems. *J. Volc. Geotherm. Res., 23,* 299-335.

Arnórsson, S., Gunnlaugsson, E., and Svavarsson, H., 1983: The chemistry of geothermal waters in Iceland II. Mineral equilibria and independent variables controlling water compositions. *Geochim. Cosmochim. Acta, 47,* 547-566.

Arnórsson, S., Sigurdsson, S. and Svavarsson, H., 1982: The chemistry of geothermal waters in Iceland I. Calculation of aqueous speciation from 0°C to 370°C. *Geochim. Cosmochim. Acta, 46,* 1513-1532.

Bjarnason, J.Ö., 1994: *The speciation program WATCH, version 2.1.* Orkustofnun, Reykjavík, 7 pp.

Craig, H., 1961a: Isotopic variations in meteoric water. *Science, 133*, 1702-1703.

Craig, H., 1961b: Standards for reporting concentrations of deuterium and oxygen-18 in natural waters. *Science 133*, 1833-1834.

Fournier, R.O., 1973: Silica in thermal waters. Laboratory and field investigations. *Proceedings of the International Symposium on Hydrogeochemistry and Biochemistry, Tokyo, 1, Clark Co., Washington D.C.,* 122-139.

Fournier, R.O., 1977: Chemical geothermometers and mixing model for geothermal systems. *Geothermics, 5,* 41-50.

Fournier, R.O., 1979: Geochemical and hydrologic considerations and the use of enthalpy-chloride diagrams in the prediction of underground conditions in hot spring systems. *J. Volc. & Geoth. Res., 5,* 1-6.

Fournier, R.O., 1991: Water geothermometers applied to geothermal energy. In: D'Amore, F. (coordinator), *Application of geochemistry in geothermal reservoir development.* UNITAR/UNDP publication, Rome, 37-69.

Giggenbach, W.F., 1988: Geothermal solute equilibria. Derivation of Na-K-Mg-Ca geoindicators. *Geochim. Cosmochim. Acta, 52,* 2749-2765.

Giggenbach, W.F., 1991: Chemical techniques in geothermal exploration. In: D'Amore, F. (coordinator), *Application of geochemistry in geothermal reservoir development.* UNITAR/UNDP publication, Rome, 119-142.

Giggenbach, W.F., 1992: Isotope shift in waters from geothermal and volcanic systems along convergent plate boundaries and their origin. *Earth and Planetary Sci. Lett., 113*, 495-510.

Libby, W.F., 1949: *Radiocarbon dating.* University of Chicago Press, Chicago.

Pan Xiaoping, 1995: *Feasibility report on developing geothermal resources in the northeastern part of the Xiaotangshan geothermal field.* Beijing Geologic Engineering Survey Institute.

Pan Xiaoping, 1996: *Feasibility report on reinjection test using waste water from geothermal space heating in the Xiaotangshan geothermal field.* Beijing Geologic Engineering Survey Institute.

Pan Xiaoping, Zeng Ruixiang, and Tian Zhenhe, 1997: *Exploration report of the Xiaotangshan geothermal field, Beijing.* Beijing Geologic Engineering Survey Institute.

Sveinbjörnsdóttir, Á.E., Heinemeier, J., and Arnórsson, S., 1995: Origin of ^{14}C in Icelandic groundwater. In: Cook G.T., Harkness, D.D., Millerand, B.F., and Scott, E.M. (editors), *Proceedings of the 15th Radiocarbon Conference. Radiocarbon, 37,* 551-565.

Truesdell, A.H., 1991: Effects of physical processes on geothermal fluids. In: D'Amore, F. (coordinator), *Application of geochemistry in geothermal reservoir development.* UNITAR/UNDP publication, Rome, 71-92.

Zheng K., 1991: Simulation and forecast of change due to exploitation of a geothermal water regime. *Proceedings of the 13th New Zealand Geothermal Workshop, University of Auckland,* 81-84.

Zheng K., Pan Xiaoping, Tian Zhenhe, and Wang Zhi, 1997: Changes in hydrogeochemistry during the development of the Xiaotangshan geothermal field, Beijing, China. *Proceedings of the 19th New Zealand Geothermal Workshop, University of Auckland,* 105-108.